Simultaneous Notch Filtering and Linearization in an Integrated Microwave Photonic Circuit

Gaojian Liu[1,2], Okky Daulay[1], Qinggui Tan[2], Hongxi Yu[2], Marcel Hoekman[3], Edwin J. Klein[3] and David Marpaung[1]
[1]Nonlinear Nanophotonics Group, University of Twente, Enschede, Netherlands
Email: g.liu@utwente.nl, o.f.p.daulay@utwente.nl, david.marpaung@utwente.nl
[2]China Academy of Space Technology, Xi'an, China
[3]LioniX International BV, Enschede, Netherlands

2021 International Topical Meeting on Microwave Photonics (MWP) | 978-1-6654-2610-7/21/$31.00 ©2021 IEEE | DOI: 10.1109/MWP53341.2021.9639413

***Abstract*—We demonstrated, for the first time, an integrated microwave photonic (MWP) circuit exhibiting simultaneous tunable notch filtering and linearization, leading to a high performance filter with enhanced linearity and spurious free dynamic range (SFDR). We unlock this unique feature by manipulating the phase and amplitude of multi-order RF modulation sidebands using a versatile MWP spectral shaping circuit. Through a series of experiments, we show a linearized notch filter that exhibits a stopband rejection of 53 dB, more than 32 dB reduction of third-order intermodulation distortion in the passband, and an enhanced SFDR of 119 $dB \cdot Hz^{2/3}$. Our demonstration breaks the conventional and fragmented approach of functionality and linearization in integrated circuit and will potentially stimulate the implementation of integrated MWP system with advanced functionalities and high performance in the future.**

***Keywords*—integrated microwave photonics, notch filter, linearization, spectral shaping**

I. Introduction

With the convergence of photonic integrated circuits (PICs) and microwave photonics (MWP), integrated MWP becomes a fast growing technology to process high frequency microwave signal, which enables complex advanced functionalities with reduced footprint and improved stability [1]. Plenty of MWP signal processing subsystems have been demonstrated on chip, like phase shifting [2] beamforming [3] and filtering [4]–[6], which are promising counterparts to break the electronic bottlenecks in microwave engineering.

While advances in integrated MWP are encouraging, the field now is still largely fragmented. Many approaches look only at providing functions in integrated devices, but entirely neglect the system RF performance [2]–[4]. Recent works have focused on combining functions with reduction of noise figure through optical carrier processing [7], [8], but linearization methods, which are critical for achieving high spurious free dynamic range (SFDR), are largely absent in integrated MWP devices. We have recently demonstrated that linearization can be done in a photonic chip through advanced MWP spectral shaping [9]. The basic idea is tailoring the phase and amplitude of optical carrier and multi-order sidebands to make the third-order intermodulation distortion (IMD3) terms from different beating products destructively interfered [9], [10].

This work was supported by Netherlands Organisation for Scientific Research NWO Vidi (15702) and Start Up (740.018.021). G. Liu was supported by Chinese Scholarship Council.

With this work, we aim to show that it is possible to combine MWP functionalities and linearization in the same PIC, demonstrating for the first time an integrated MWP filter with enhanced linearity and SFDR. This linearized MWP filter is achieved by vectorially manipulating the modulated optical spectrum using a novel integrated MWP spectral shaper [11]. The proposed MWP notch filter shows a rejection ratio of 53 dB, and an improved SFDR of 119 $dB \cdot Hz^{2/3}$.

II. Operation Principle

The schematic of the proposed MWP notch filter is depicted in Fig. 1. The key component for signal processing is the integrated MWP spectral shaper which consists two main parts, the modulation transformer (MT) and the tunable all-pass ring resonator. The MT is composed of a spectral de-interleaver implemented as MZI loaded with 3 ring resonators, a tunable attenuator, a phase shifter and a combiner[11]. This circuit can be used to manipulate the phase and amplitude of modulated optical spectrum to create various modulation formats, such as single sideband (SSB) modulation, phase modulation, intensity modulation, and asymmetric double sideband modulation with arbitrary phase relation [8], [11]. The all-pass ring resonator can be configured in different coupling states and resonance frequencies to precisely tailor the phase and amplitude of the optical spectrum for functionalities [12].

We first explain the operation principle of the notch filter and linearity enhancement separately and then describe the entire working flow of the linearized MWP notch filter. The notch filter is based on the destructive interference between upper sideband and lower sideband at designated frequency[4], as shown in Fig. 2 (a). In this case, only first order sidebands are taken into account. Ideally, the MT processes the phase modulated spectrum to generate asymmetric double sidebands with π-phase difference. An all-pass ring resonator at under coupling (UC) state is aligned at the stronger sideband to equalize these sidebands amplitudes and maintain the anti-phase relation at resonance frequency, as the UC ring imposes zero phase shift to the spectrum at resonance. After photodetection, a high rejection RF notch filter is achieved, as the signal from upper sideband and lower sideband are destructively interfered at the resonance frequency of ring resonator.

Authorized licensed use limited to: UNIVERSITY OF TWENTE.. Downloaded on January 12,2022 at 07:49:09 UTC from IEEE Xplore. Restrictions apply.

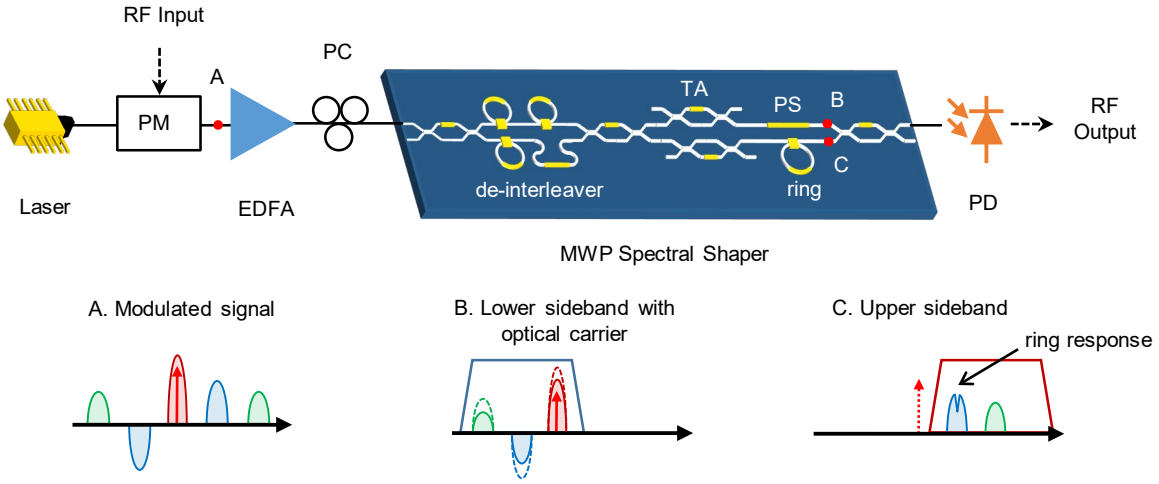

Fig. 1. Schematic of the proposed linearized MWP notch filter and the optical spectra at different positions of the system. PM, phase modulator; PC, polarization control; EDFA, erbium-doped fiber amplifier; TA, tunable attenuator; PS, phase shifter; PD, photodetector.

The linearization, on the other hand, is achieved by manipulating the power ratio between the optical carrier band (OCB) and the multi-order optical sidebands (OSB) in a phase modulation spectrum to make all the IMD3 contributors add up destructively, as shown in Fig. 2 (b). OCB contains the optical carrier and even order nonlinear distortion. ±1 OSBs are composed of fundamental signal and odd order nonlinear distortion. ±2 OSBs contain the second order harmonics and even order nonlinear distortion. In the proposed scheme, the OCB is attenuated together with the lower sideband to meet the power ratio condition for linearization and generate the asymmetric double sidebands simultaneously.

To find the proper attenuation at the lower sideband and OCB for linearization, we analyze the relation between the frequency components after photodetection. When a two-tone RF signal with angular frequency of ω_1, ω_2, and voltage of V_{RF} is modulated to the optical carrier via a phase modulator (PM), the modulated optical spectrum can be expressed as

$$E_{out}(t)=\sqrt{P_i}e^{j\omega_c t}\sum_{n=-\infty}^{+\infty}\sum_{k=-\infty}^{+\infty}J_n(m)J_k(m)e^{j(n\omega_1+k\omega_2)t} \quad (1)$$

where ω_c, P_i, J_n, $m=\pi\cdot V_{RF}/V_{\pi,RF}$, and $V_{\pi,RF}$ is the angular frequency of the optical carrier, input optical power, the n-th order Bessel function of the first kind, the modulation index of PM, and the RF half-wave voltage of the PM respectively. Under small signal condition, only zero to second order sidebands are taken into account for approximation.

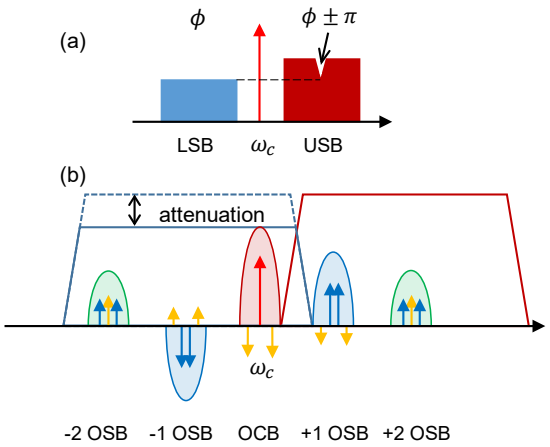

Fig. 2. (a) Operation principle of the notch filter. (b) Operation principle of linearization.

The optical spectrum after processing can be written as

$$E_p(t)=\sqrt{P_i}e^{j\omega_c t}\cdot\begin{Bmatrix}\sqrt{A}\cdot J_0J_0\\+\sqrt{A}\cdot J_{-1}J_1\left[e^{-j(\omega_1+\omega_2)t}+e^{j(\omega_1+\omega_2)t}\right]\\+J_0J_1\left(e^{j\omega_1 t}+e^{j\omega_2 t}\right)\\+J_{-1}J_2\left[e^{j(2\omega_1-\omega_2)t}+e^{j(2\omega_2-\omega_1)t}\right]\\+\sqrt{A}\cdot J_{-1}J_0\left(e^{-j\omega_1 t}+e^{-j\omega_2 t}\right)\\+\sqrt{A}\cdot J_{-2}J_1\left[e^{-j(2\omega_1-\omega_2)t}+e^{-j(2\omega_2-\omega_1)t}\right]\\+J_0J_2\left(e^{j2\omega_1 t}+e^{j2\omega_2 t}\right)\\+J_1J_1e^{j(\omega_1+\omega_2)t}\\+\sqrt{A}\cdot J_{-2}J_0\left(e^{-j2\omega_1 t}+e^{-j2\omega_2 t}\right)\\+\sqrt{A}\cdot J_{-1}J_{-1}e^{-j(\omega_1+\omega_2)t}\end{Bmatrix} \quad (2)$$

where $J_n=J_n(m)(n=0,\pm1,\pm2)$, $J_{-n}=(-1)^nJ_n$. A is the power attenuation to the lower sideband and the OCB.

The RF signal retrieved from the processed optical field can be expressed as

$$\begin{aligned}I_{PD}(t)&=R_{PD}|E_p(t)|^2\\&=I_1\cos\omega_{1,2}t+I_3\cos(2\omega_{1,2}-\omega_{2,1})t\end{aligned} \quad (3)$$

where R_{PD} is responsivity of photodetector, I_1 and I_3 are the coefficients for fundamental signal and IMD3 components, which can be expressed as

$$I_1\propto(\sqrt{A}-A)J_0^3J_1+(1-\sqrt{A})J_0J_1^3+(1-A)J_0^2J_1J_2 \quad (4)$$

$$I_3\propto(A-\sqrt{A})J_0J_1^3+(1-\sqrt{A})J_0^2J_1J_2 \quad (5)$$

When $m\ll1$, $J_n(m)\approx m^n/(2^n n!)$, I_1 and I_3 can be written as

$$I_1\propto(\sqrt{A}-A)m \quad (6)$$

Authorized licensed use limited to: UNIVERSITY OF TWENTE.. Downloaded on January 12,2022 at 07:49:09 UTC from IEEE Xplore. Restrictions apply.

$$I_3 \propto (2A - 3\sqrt{A} + 1)m^3 \tag{7}$$

To minimize the IMD3 distortion while maximizing the fundamental RF signal, the attenuation imposed to the lower sideband and OCB need to satisfy the condition:

$$\begin{cases} \sqrt{A} - A \neq 0 \\ 2A - 3\sqrt{A} + 1 = 0 \end{cases} \tag{8}$$

The first condition in (8) guarantees that the fundamental RF signal can be detected after photodetection. The second condition gives the processing imposed to the modulated spectrum for IMD3 terms cancellation. There are two solutions in the second condition in (8), A=1 and A=1/4. The solution A=1 means no processing is imposed to the phase modulated spectrum, where neither fundamental signal nor IMD3 terms can be detected after photodetection. The other solution A=1/4 is the linearization condition we need, which means the optical power of lower sideband and optical carrier should be attenuated for 6 dB. In this case, the IMD3 terms are greatly reduced while the fundamental signal can still be detected.

Finally, we describe the entire working flow of the linearized MWP notch filter. The RF signal is modulated into optical domain through a phase modulator, generating an OCB and multi-order OSBs, as depicted in Fig. 1 point A. The ± 1 OSBs are out of phase with equal amplitudes. The ± 2 OSBs have equal phases and amplitudes. The modulated optical signal is coupled into an integrated MWP spectral shaper for signal processing. The spectral de-interleaver in MWP spectral shaper separates the upper sideband and lower sideband with optical carrier into two paths. The lower sideband and the OCB are processed by the tunable attenuator and phase shifter connected to one output port of the de-interleaver, as shown in Fig. 1 point B. The attenuator adjusts the power ratio between the OCB with the lower sideband and the upper sideband to meet the linearization condition and generates the asymmetric double sidebands for notch filter. The phase shifter maintains the phase relation of the lower sideband and the upper sideband as phase modulation, when the signals in two paths are recombined. A ring resonator at under coupling state is used to process the stronger sideband, as shown in Fig. 1 point C. When the equal amplitude and anti-phase requirements at two first order sidebands are satisfied, a linearized notch filter is achieved after photodetection.

III. Experiment Results

A proof of concept experiment is performed to verify the feasibility of the proposed linearized notch filter. The setup is illustrated in Fig. 1 (a). An optical carrier with the power of 18 dBm and wavelength of 1550.054 nm from a continuous-wave (CW) laser (Pure Photonics PPCL550) is modulated by a phase modulator (PM, EOSpace 20 GHz). The sweeping RF signal with -3 dBm power from vector network analyzer (VNA, Keysight P9375A) is used to drive the PM for filter response measurement. The two-tone RF signal located at frequency of 9 GHz and 9.01 GHz with power of 3.5 dBm from signal generators (Wiltron 69147A and Rohde-Schwarz SMP02) is modulated to the optical carrier via the PM for linearity measurement. After amplified by a low noise erbium-doped fiber amplifier (EDFA, Amonics), the modulated optical signal is coupled to a programmable silicon nitride chip (LioniX International) for processing. The chip has a coupling loss of 1.5 dB per facet and propagation loss of 0.1 dB/cm in straight waveguide. The de-interleaver has a 3 dB bandwidth of 80 GHz, and an FSR of 160 GHz. The rejection in stopband is 25 dB. The 3 dB-to-25 dB transition is measured as 2.5 GHz which is equivalent to 1.6% of the FSR. The tunable ring resonator used to create notch response has an FSR of 50 GHz. The processed optical spectrum is then sent to a photodetector (EMCORE 20GHz) to retrieve RF signal. The RF signal after photodetection is sent to the VNA and the RF spectrum analyzer (Keysight N9000B) to measure the filter response and linearity.

There are two sets of measurement performed in the experiment for comparison. One is the proposed linearized notch filter where the MWP spectral shaper processes the phase modulated spectrum to meet the condition for linearization and notch filter. The other is a conventional SSB notch filter without linearization as a benchmark, in which the MT generates an SSB modulation spectrum, and the ring resonator at same coupling state as in the proposed linearized notch filter is used to process SSB signal for notch response. In two sets of measurement, the optical power sent to photodetector are maintained as 4 dBm.

The response of the proposed linearized notch filter and the conventional SSB notch filter are depicted in the Fig. 3. (a).

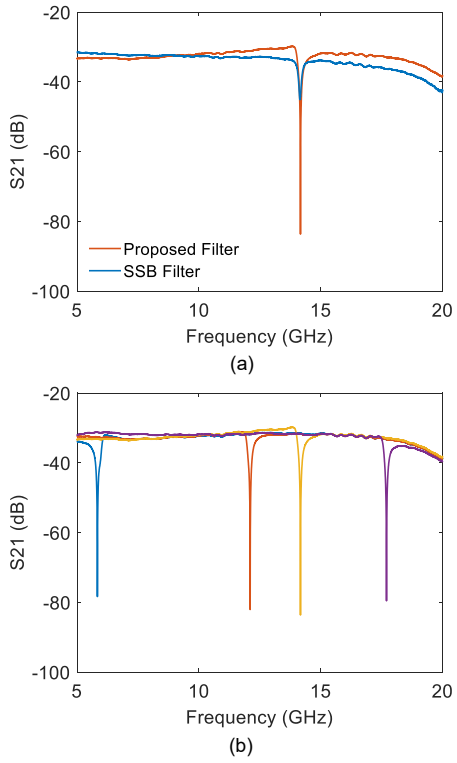

Fig. 3. (a) Filter response of the proposed scheme and the SSB scheme. (b) Frequency tuning of proposed notch filter.

Authorized licensed use limited to: UNIVERSITY OF TWENTE.. Downloaded on January 12,2022 at 07:49:09 UTC from IEEE Xplore. Restrictions apply.

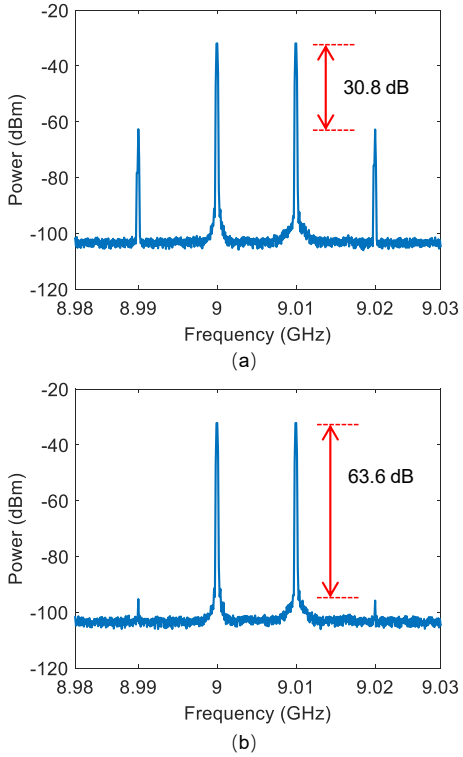

Fig. 4. Retrieved RF spectra under two-tone test. (a) RF spectrum from SSB notch filter. (b) RF spectrum from linearized notch filter.

The proposed notch filter exhibits a high stopband rejection of 53 dB which has more than 40 dB enhancement compared with the SSB notch filter using the same ring resonator. This high rejection is due to the destructive interference between two optical sidebands. The frequency tunability of the proposed filter is illustrated in Fig. 3 (b). The filter can be tuned from 6 GHz to 18 GHz with a rejection in the stopband of more than 45 dB in the entire tunning range. The retrieved RF spectra under two-tone test from SSB notch filter and proposed linearized notch filter are shown in Fig 4. (a) and (b) respectively. The fundamental to IMD3 ratio (FIR) is 30.8 dB in SSB filter. In linearized filter the FIR is increased to 63.6 dB. More than 32 dB IMD3 suppression is observed.

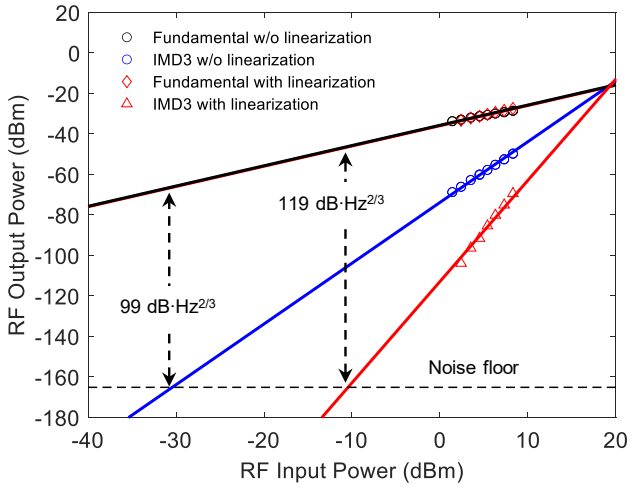

Fig. 5. Measured SFDR of the linearized filter and SSB filter without linearization.

The SFDR of the proposed notch filter is measured and compared with the conventional SSB notch filter, as shown in Fig. 5. With a noise floor of -165.1 dBm/Hz, the conventional SSB notch filter has an SFDR of 99 $dB{\cdot}Hz^{2/3}$. The linearized filter exhibits a much larger SFDR of 119 $dB \cdot Hz^{2/3}$. This significant 20 dB improvement comes from the large suppression of the IMD3.

IV. Conclusion

We demonstrate, for the first time, a tuneable MWP notch filter with enhanced linearity. The notch filter can be tuned from 6 GHz to 18 GHz, with a maximum stop band rejection of 53 dB. The SFDR of the linearized filter is measured as $119dB \cdot Hz^{2/3}$, which is 20 dB larger than the conventional SSB notch filter. The filter functionality and linearization are achieved simultaneously by precisely tailoring the modulated optical spectrum using a MWP spectral shaper. These results point to the great potential of integrated MWP system with advanced functionality and high performance.

Acknowledgment

The authors would like to thank Power Electronics & EMC group in University of Twente for their help in measurement.

References

[1] D. Marpaung, J. Yao, and J. Capmany, "Integrated microwave photonics," Nat. Photon., vol. 13, no. 2, pp. 80–90, 2019.
[2] S. X. Chew, D. Huang, L. Li, S. Song, M. A. Tran, X. Yi, and J. E. Bowers, "Integrated microwave photonic phase shifter with full tunable phase shifting range (>360°) and RF power equalization," Opt. Exp., vol. 27, no. 10, pp. 14798–14808, May 2019.
[3] C. Zhu, L. Lu, W. Shan, W. Xu, G. Zhou, L. Zhou, and J. Chen, "Silicon integrated microwave photonic beamformer," Optica, vol. 7, no. 9, pp. 1162–1170, Sep. 2020.
[4] D. Marpaung, B. Morrison, R. Pant, C. Roeloffzen, A. Leinse, M. Hoekman, R. Heideman, and B. J. Eggleton, "Si3N4 ring resonator-based microwave photonic notch filter with an ultrahigh peak rejection," Opt. Exp., vol. 21, no. 20, pp. 23286–23294, Oct. 2013.
[5] Y. Liu, J. Hotten, A. Choudhary, B. J. Eggleton, and D. Marpaung, "All-optimized integrated RF photonic notch filter," Opt Lett, vol. 42, no. 22, pp. 4631–4634, Nov. 2017.
[6] Y. Tao, H. Shu, X. Wang, M. Jin, Z. Tao, F. Yang, J. Shi, and J. Qin, "Hybrid-integrated high-performance microwave photonic filter with switchable response," Photon. Res., vol. 9, no. 8, pp. 1569–1580, Aug. 2021.
[7] O. Daulay, G. Liu, and D. Marpaung, "Microwave photonic notch filter with integrated phase-to-intensity modulation transformation and optical carrier suppression," Opt. Lett., vol. 46, no. 3, pp. 488–491, Feb. 2021.
[8] O. Daulay, G. Liu, X. Guo, M. Eijkel, and D. Marpaung, "A Tutorial on Integrated Microwave Photonic Spectral Shaping," J. Lightw. Technol, vol. 39, no. 3, pp. 700–711, Feb. 2021.
[9] G. Liu, O. Daulay, Y. Klaver, R. Botter, Q. Tan, H. Yu, M. Hoekman, E. J. Klein, and D. Marpaung, "Integrated Microwave Photonic Spectral Shaping for Linearization and Spurious-Free Dynamic Range Enhancement," J. Lightw. Technol, pp. 1–1, 2021.
[10] R. Wu, T. Jiang, S. Yu, J. Shang, and W. Gu, "Multi-Order Nonlinear Distortions Analysis and Suppression in Phase Modulation Microwave Photonics Link," J. Lightw. Technol., vol. 37, no. 24, pp. 5973–5981, Dec. 2019.
[11] X. Guo, Y. Liu, T. Yin, B. Morrison, M. Pagani, O. Daulay, W. Bogaerts, B. J. Eggleton, A. Casas-Bedoya, and D. Marpaung, "Versatile silicon microwave photonic spectral shaper," APL Photon., vol. 6, no. 3, p. 036106, Mar. 2021.
[12] W. Bogaerts, P. De Heyn, T. Van Vaerenbergh, K. De Vos, S. Kumar Selvaraja, T. Claes, P. Dumon, P. Bienstman, D. Van Thourhout, and R. Baets, "Silicon microring resonators," Laser & Photon. Rev., vol. 6, no. 1, pp. 47–73, 2012.

Authorized licensed use limited to: UNIVERSITY OF TWENTE.. Downloaded on January 12,2022 at 07:49:09 UTC from IEEE Xplore. Restrictions apply.